# DER Capacity Assessment of Active Distribution Systems Using Dynamic Operating Envelopes

Masoume Mahmoodi, Lachlan Blackhall, S. Mahdi Noori R.A., Ahmad Attarha, Ben Weise, Abhishek Bhardwaj

***Abstract*—The increasing deployment of distributed energy resources (DER) within electricity distribution systems can push them outside their safe operational limits. This urges the distribution system operators (DSO) to perform a DER capacity assessment that utilises the network's full potential to accommodate more DER while ensuring the network's safety. However, this is a challenging task as the DER units are mostly consumer-owned and therefore the DSO does not have control over them. To overcome this challenge, this paper first develops dynamic operating envelopes (DOEs). A DOE is a convex set defining acceptable real and reactive powers exchange with the grid at a consumer connection point without violating any network constraints. We propose a novel methodology to calculate a DOE by applying the right-hand side decomposition technique through which we allocate the network's capacity to mutually independent consumers. We then build a hierarchical DER capacity assessment within DOEs that considers the uncertainty of solar power and demand when making investment decisions. In the proposed framework, the consumers are then free to make their decisions as long as they comply with their DOEs.**

***Index Terms*—Dynamic operating envelope, distributed energy resources, DER capacity assessment, unbalanced distribution systems, right-hand side decomposition.**

## I. Introduction

Global power systems are undergoing a significant transition from centralised fossil fuel-based generation to emission-free renewable energy-based distributed energy resources (DER). However, the poles and wires of electricity distribution systems have not been designed for such a setting, and therefore, the high integration of DER units into the network can cause violations of its operational limits. Hence, it is essential to perform a DER capacity assessment of an active distribution system to utilise its full potential while still ensuring its safety.

There is a vast body of literature on DER capacity assessment of active distribution systems. Most of these studies, e.g. [1]–[6], assume that a central entity, commonly the distribution system operators (DSO), has full visibility and controllability over the already-installed or to-be-installed assets across the grid. However, these assets are typically owned by consumers and therefore installed behind their meters, where based on the current regulations in most countries, the DSO is not allowed to control directly. Studies like [7]–[11] acknowledge consumers' freedom in managing their own assets. However, they either $i$) employ a distributed optimisation approach, e.g. ADMM as in [7], [8], which suffer from slow convergence, or $ii$) often fail to maintain grid's safety as they either consider static limits on their export or overly simplified controllers, such as volt-var controllers within consumer problems [9], [10]. In our previous work [11], we assessed the effectiveness of such local control approaches in the DER hosting capacity problem and observed that they could not guarantee the grid's safe limits and underestimated the network's DER capacity.

In this paper, we propose a hierarchical framework for DER capacity assessment in active distribution systems. Our approach is to decompose the central problem into network and consumer problems and solve their optimisation problems in sequential order. First, the DSO solves the network problem which outputs *dynamic operating envelopes (DOEs)*[1]. A DOE is defined as a convex set including an acceptable range of real and reactive power flows for each consumer's connection point that ensures the safe operation of the network within each operational interval. Then, each consumer optimises for their DER installation capacity (we consider PV and battery storage systems in our study) while integrating the DOEs received from the network as constraints into their optimisation problem. Therefore, unlike central approaches that assume full controllability of consumer-owned assets, our proposed DOE-based framework provides consumers with more agency on how to manage their assets (install a new asset or operate the available ones). Also, compared to iterative distributed approaches, e.g., [7], [14], our framework does not have any convergence issues as it is not based on iterative algorithms while not underestimating the grid's capacity to host more DGs.

We ensure that our approach is robust to uncertainty by developing local controllers that allow consumers to compensate for their uncertainty such that their connection point power is within their allocated DOEs. This ensures that uncertainty does not jeopardise the network's safety. This is different from distributed optimisation-based approaches like [14], as here, we do not require to iterate several times between the consumer and master problem to achieve a consensus solution. However, similarly to the distributed optimisation-based approaches, our approach can reach the same solution as the original problem.

The remainder of this paper is organised as follows. Section II provides a literature review and discusses the motivations behind our work. Section III introduces our proposed methodology to calculate DOEs. Section IV details the hierarchical DER capacity assessment model. Numerical results and discussion are provided in Section V. Finally, the paper is concluded in Section VII.

Authors are with the College of Engineering and Computer Science, The Australian National University (ANU), Canberra, Australia. Emails: firstname.lastname@anu.edu.au

[1]DOE approach was introduced by the authors as part of the EVOLVE project [12], [13] to increase the market participation of distributed energy resources without violating the network's constraints.

## II. Related Work and Literature Gap

At the moment, the DOE notion is in its infancy, and little research has been done on calculating and utilising these DOEs for operation and planning purposes. There is a stream of literature investigating an operational flexibility region, mostly for the intersection of distribution and transmission systems. In [15], [16], a flexibility area containing real and reactive power limits at the TSO[2]/DSO boundary node is calculated by performing multiple optimal power flows (OPFs). In [17], the authors determine the capability area of an active distribution system to provide both real and reactive power reserves. Similarly, [18] develops an AC OPF-based methodology to generate a real-reactive power (PQ) capability chart, which characterises the short-term flexibility capability of active distribution networks to provide ancillary services to TSO. Although these flexibility regions are network-aware and therefore guarantee the network's safety, they mainly have two issues; first, they only obtain one flexibility region for the TSO/DSO boundry node and second, their inherent assumption is that the DSO has full observability and controllability of the consumer-owned flexible distributed energy resources (DER). In this paper, we overcome these issues by obtaining DOEs for each DER-owned consumer's connection point while allowing consumers to operate their DER as they wish as long as their connection point power remains within their DOE.

At the distribution system level, the authors in [9] explored day-ahead, time-varying real power export limits for each flexible consumer and compared these dynamic limits with the fixed static export limits from both network's and consumers' perspectives. Recently, [19] has developed a framework for the DSO to determine the real power dynamic limits for each node if a potential violation is detected as a result of requested power flows by the consumers or aggregators. However, they assume full observability of consumer-owned DER by DSO, which is not available in practice. Also, both [9], [19] have neglected the reactive power flexibility / support that can be provided by grid-connected inverters. The authors in [14] proposed network-secure operating envelopes that facilitate the participation of consumers in energy and reserve markets. However, the envelopes in [14] cannot guarantee the network's limits for unbalanced networks. Plus, they do not provide any region for reactive power and consumers are forced to inject / absorb reactive power based on a pre-determined function.

Another issue with the studies on DOE is that they often over-simplify the behind-the-meter problem, as they either $i$) ignore the uncertainties associated with DER units and electrical demand on the consumer side [9], [19], [20], or $ii$) overlook the capability of fast-acting devices, such as inverters, in responding to uncertainties once they are revealed [2], [3]. To have a DER capacity assessment that neither under nor over-estimates DER installation capacity, it is important to account for these uncertainties as well as the recourse capability of inverters.

To overcome the above-mentioned issues, this paper presents a DER capacity assessment that not only accounts for uncertainties and recourse capability of inverters but provides consumers with more agency to take their investment and operation decisions. This is unlike our previous work [4], where a DSO centrally schedules the behind-the-meter devices. At the heart of our proposed framework lies a DOE calculation methodology which provides a joint real and reactive power feasible region for each flexible node within each operational interval, and it is applicable in both balanced and unbalanced three-phase active distribution systems. To determine DOEs, we (or DSO) employ the right-hand side (Kornai–Liptak) decomposition technique [21], [22]. In this technique, the main idea is that the global optimal value in a complex system can be achieved by some allocation procedure of joint resource shares between mutually independent sectors (consumers in our problem), whereas sectors are free in choosing their actions. By leveraging this technique, we demonstrate a convex reformulation of the hosting capacity calculation problem in electrical distribution systems. This reformulation brings mathematically proven advantages to our modelling, including scalability with polynomial solve time and the ability to guarantee a globally optimal solution [23]. The DSO can employ any objective function to determine the share of each consumer, and consequently its DOE, while still preserving the global optimal solution inside the consumers' feasible regions.

On the consumer side, we address the uncertainties of distributed energy resources (DER) output and demand by implementing the adjustable robust counterpart (ARC) methodology [24]. This approach enables real-time adjustment of fast-acting devices by optimising the parameters of affine functions that take uncertainty as input and provide the devices' response as output. In our modelling, each consumer determines their DER installation capacity while optimising affine functions for both the real and reactive power output of PV and battery storage systems. This optimisation allows for live recourse actions to be taken once the uncertainty is realised.

The major contributions of this work are:

- A novel methodology to calculate a dynamic operating envelope (DOE). Unlike [9], [19] that have neglected the reactive power flexibility / support that can be provided by inverters, our DOE provides the acceptable range for both real and reactive powers. Contrary to [14], our DOE calculation methodology is suitable for both balanced and unbalanced networks. This is important as most distribution systems are inherently unbalanced. Moreover, unlike [15]–[18] that obtain a flexibility region at the TSO/DSO boundary node, we allocate the distribution system capacity between the consumers. Our approach decentralises from the top-down, where the DSO provides consumers with a network-secure PQ region. In contrast, the approaches mentioned above look at decentralisation from the bottom-up, starting from behind the connection point (in their case, the distribution system) and requiring behind-the-meter information.
- A hierarchical framework for DER capacity assessment of active distribution systems using DOEs. Firstly, the DSO calculate and send the DOEs to consumers, and then, each consumer optimises for their DER installation capacity while integrating the DOEs received from the network as constraints into their optimisation problem.

[2]Transmission system operators.

Unlike [1]–[3], our framework provides consumers with more agency on how to schedule their flexible assets, instead of allowing the DSO to directly control their assets. In our framework, the feasible region of the distributed problem contains the optimal operating point of the original problem and does not compromise that. Therefore, our approach has the potential to achieve the network's optimal solution without requiring central control and coordination.

## III. Proposed Methodology to Calculate Dynamic Operating Envelopes

### A. Modelling Notation

*Distribution Network:* A three-phase distribution system can be represented using graph $\mathcal{G}=(\mathcal{V},\mathcal{E})$, where $\mathcal{V}=\{0,...,\mathrm{N}\}$ denotes the set of all nodes and $\mathcal{E}\subseteq\mathcal{V}\times\mathcal{V}$ is the set of all edges. Node 0 is considered as the slack node, and it is connected to the upstream network. Let $\Phi=\{a,b,c\}$ denote the set of all phases, and $\mathcal{T}$ denote the set of all time intervals. Also, let set $\mathcal{V}_c:=\mathcal{V}_g\cup\mathcal{V}_{g'}$ denote all the nodes and phases with power consumption and / or injection, i.e., the connection points that supplies consumers. We then define the set of connection points that wish to install a DER system, i.e., the nodes that we want to assign a DOE to them, by $\mathcal{V}_g$, and the rest of the connection points by $\mathcal{V}_{g'}$. We also define the set of participant consumers and non-participant consumers by $\mathcal{L}:=\{1,...,L\}$ and $\mathcal{L}':=\{1,...,L'\}$ where $L$ and $L'$ are the total numbers of participant and non-participant consumers, respectively. Note that sets $\mathcal{V}_g$ and $\mathcal{L}$ are equivalent (similarly, consumer $\ell\in\mathcal{L}$ is equivalent to $(j,\varphi)\in\mathcal{V}_g$) and will be used interchangeably throughout the paper for ease of exposition. For node $j$ and phase $\varphi$ at the time interval $t$, let $V_{j\varphi t}$, $p_{j\varphi t}$ and $q_{j\varphi t}$ denote the complex voltage, net real and reactive power injections. Also, let $P_{ij,\varphi t}$ and $Q_{ij,\varphi t}$ denote the real and reactive power flows in the edge $(i,j)$ and phase $\varphi$ at time interval $t$.

*Consumer:* For behind the connection point of each participant consumer's premises (behind-the-meter), we define:

$$p_{\ell t}:=-p^{d}_{\ell t}+p^{der}_{\ell t},\quad q_{\ell t}:=-q^{d}_{\ell t}+q^{der}_{\ell t},\qquad \forall\ell\in\mathcal{L},\quad (1)$$

where superscript $d$ refers to passive demand, and $der$ refers to the flexible powers provided by DERs. Additionally, we define the size of an installed DER system as $G^{der}_{\ell}$.

Similarly, the net real and reactive power injection of the non-participant consumers are defined as follows:

$$p_{\ell t}:=-p^{d}_{\ell t},\quad q_{\ell t}:=-q^{d}_{\ell t},\qquad \forall\ell\in\mathcal{L}'.\qquad (2)$$

Notice that the parameters $p^{d}_{\ell t}$ and $q^{d}_{\ell t}$ in (2) can have positive or negative values as these consumers may have already installed a DER behind their meter.

### B. The Need for DOE

A DER capacity assessment can be characterised by the following general central optimisation model:

$$\min_{\boldsymbol{x}}\ \mathbb{C}(\boldsymbol{x}) \qquad (3a)$$

$$s.t.\quad \mathrm{g}(\boldsymbol{x},\boldsymbol{\xi})\leq 0 \qquad (3b)$$

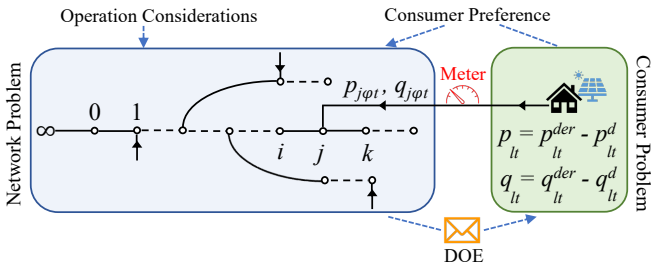


Figure 1. Architecture of the proposed decomposition where network and consumer problems are only connected through DOEs.

where $\boldsymbol{x}:=[G^{der}_{\ell},p^{der}_{\ell t},q^{der}_{\ell t}]\ \forall\ell\in\mathcal{L},t\in\mathcal{T}$ and $\boldsymbol{\xi}$ represent the vector of decision variables and problem parameters, respectively. This model minimises the generic function $\mathbb{C}$, such that the physical limits of the network and DERs, shown by the generic function $\mathrm{g}$, are satisfied. The specific form of the function $\mathbb{C}$ depends on the goals of the system operators and consumers with respect to operating DER units within the power system. In other words, function $\mathbb{C}$ can be tailored to meet the specific needs and objectives of the stakeholders involved. Examples of $\mathbb{C}$ are maximising social welfare, minimising system losses and maximising the network's real power throughput. The details of these functions will be further investigated in Section IV.

The assumption of the central model (3) is that the DSO has full visibility and controllability over all consumers' assets. To provide consumers with an agency to make their investment and operation decisions, we propose to decompose the central optimisation problem (3) into one network problem and multiple consumer problems (one for each consumer) where their connection is through DOEs. The architecture of this decomposition is shown in Fig. 1. As can be seen, in this structure, the network operator does not have access to the behind-the-meter of each consumer but rather guarantees the network's safety through a range of acceptable powers, i.e., DOE, for the connection point of each consumer. In the following sections, we first formally define a DOE and describe the network problem used by us (or the DSO) to calculate the DOEs. We then explain the consumer problems and how they use their DOEs to determine their investment (DER capacity) and operation (inverter's set point and battery operation) decisions.

### C. DOE Definition

For each consumer connected to node $j$ and phase $\varphi$, we define a DOE within each time interval $t$ as:

**Definition 1** (DOE)**.** A DOE is defined by a nonempty, convex and closed set $\boldsymbol{\Omega}_{\ell t}\subseteq\mathbb{R}^2$ in the $(p_{\ell t},q_{\ell t})$ coordinates which characterises the range of real and reactive power flows for this node that can be safely accommodated by the distribution network within time interval $t$.

An example of a DOE is shown in Fig. 2. The consumer can take on any operating point inside the gray region without negatively affecting the network's operational constraints. Therefore, DOE approach enables DSO to ensure safety of the

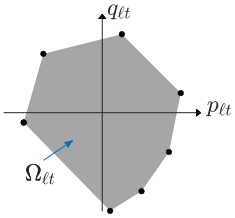


Figure 2. An example of a DOE issued to consumer $\ell$ within time interval $t$.

network without directly controlling the consumers. The DOEs need to be calculated by DSO for each operating interval (e.g. hourly or 5-minute interval) and sent to the consumers in advance (e.g. day-ahead for operation and year-ahead for planning purposes).

### *D. Network Problem: DOE Calculation*

In this section, we introduce the network problem and propose a novel methodology to determine the DOEs.

To have a safe operation, the DSO needs to periodically ensure that the physical limits of the network, e.g., voltage and thermal limits, are satisfied. Additionally, the DSO might consider additional constraints to account for other considerations like consumers preferences. Considering these constraints, the network problem in DER capacity assessment can be written as:

$$\min_{\Xi_{\mathcal{N}}} \ \mathbb{C}^{net}(\mathbf{p},\mathbf{q}), \quad s.t. \tag{4a}$$

$$\Xi_{\mathcal{N}} := \{p_{j\varphi t}, q_{j\varphi t}, \forall (j,\varphi) \in \mathcal{V}_g, t \in \mathcal{T} \mid f(\mathbf{p},\mathbf{q}) \leq \mathbf{b}\}, \tag{4b}$$

where $\Xi_{\mathcal{N}} \subseteq \mathbb{R}^{2L\times T}$ denotes the network's feasible set with $L$ representing the total number of consumers and $T := |\mathcal{T}|$ denoting the total number of time intervals. Also, parameter $\mathbf{b}$ is known and determined using the network's acceptable limits. Vectors $\mathbf{p}$ and $\mathbf{q}$ collect real and reactive power injections of all consumer nodes. The objective function $\mathbb{C}^{net}$ minimises the network operator's goal using only in-front-of-the-meter information, i.e., the consumers' real and reactive power injections to the grid denoted by $\mathbf{p}$ and $\mathbf{q}$. Notice that in our modelling, the DSO does not require access to information about appliances behind the meter, nor does it need to make decisions regarding their operation. Thus, our modelling preserves the consumers' agency. Also, note that the network operator's objective is not necessarily the same as the consumers'. In Sections III-E and V, we will discuss the impact of having different objectives for the network and consumers. Moreover, function $f$ in (4) includes the network's constraints (e.g. voltage and thermal constraints). Let us denote the output of the network optimisation model (4) with $\Xi^*_{\mathcal{N}} := \{p^*_{j\varphi t}, q^*_{j\varphi t}, \forall (j,\varphi) \in \mathcal{V}_g, t \in \mathcal{T}\}$.

Since power systems are interconnected systems, the feasible region of each grid-connected consumer inherently depends on the behaviour of others in the system. However, in practice there is either no or very limited communication structure available in current distribution systems[3]. To overcome this limitation, we propose to disaggregate the $2LT$-dimensional feasible region $\Xi_{\mathcal{N}}$ into $LT$, two-dimensional independent regions defined as DOEs:

$$\Xi_{\mathcal{N}} \rightarrow \underbrace{\mathbf{\Omega}_{11},...,\mathbf{\Omega}_{1T}}_{\text{consumer 1}},...,\underbrace{\mathbf{\Omega}_{L1},...,\mathbf{\Omega}_{LT}}_{\text{consumer L}}, \tag{5}$$

where $\mathbf{\Omega}_{\ell t} \subseteq \mathbb{R}^2, \forall \ell \in \mathcal{L} := \{1,...,L\}, t \in \mathcal{T}$ represents the feasible region of consumer $\ell$ within time interval $t$. Let us assume that consumer $\ell$ is located at node $j$ and phase $\varphi$ and therefore $\mathbf{\Omega}_{\ell t} = \mathbf{\Omega}_{j\varphi t}$. With disaggregation (5), we can obtain the feasible region of each consumer within each time interval. The feasible region of the disaggregated problem denoted by $\mathbf{\Omega} : \mathbf{\Omega}_{11} \times \cdots \times \mathbf{\Omega}_{LT} \subseteq \Xi_{\mathcal{N}}$ is the Cartesian product of the independent DOEs and it is a subset of the network's feasible set. In what follows, we describe the details of our proposed disaggregation and consequently DOE determination.

We utilise the separable structures of the network's constraints, as will be detailed in Section IV, and re-express them in the following form:

$$\sum_{\ell=1}^{L} f_\ell(p_{\ell t}, q_{\ell t}) \leq b_t, \quad \forall t \in \mathcal{T}, \tag{6}$$

where $f_\ell : \mathbb{R}^2 \rightarrow \mathbb{R}^m$ is a linear vector function with components $f_{\ell,h} : \mathbb{R}^2 \rightarrow \mathbb{R}$ for $h = 1,...,m$, where $m$ is the total number of network's constraints within time interval $t$. The properties of this function depends on the characteristics of the network (e.g. branch impedances and the topology of the network). Also, parameter $b_t \in \mathbb{R}^m$ is known and determined using the network's acceptable limits.

We then employ the right-hand side decomposition (RHSD) approach [21], [22]. In the RHSD approach, the main idea is that the optimal solution of a complex system can be achieved by some allocation procedure of joint resource shares between mutually independent sectors, where sectors are free to choose their actions. In the context of our problem, sectors are consumers, and the joint resources are the network's constraints. Based on this approach, for each consumer $\ell$, we determine a partition $w_{\ell t}$ of the right-hand side vector $b_t$ such that:

$$\sum_{\ell=1}^{L} w_{\ell t} = b_t, \quad \forall t \in \mathcal{T}, \tag{7}$$

where $w_{\ell t} \in \mathbb{R}^m$ represents the contribution of consumer $\ell$ in satisfying the network's constraints at time interval $t$. Substituting (7) in the constraint (6) gives:

$$\sum_{\ell=1}^{L} f_\ell(p_{\ell t}, q_{\ell t}) \leq \sum_{\ell=1}^{L} w_{\ell t}, \quad \forall t \in \mathcal{T}, \tag{8}$$

which can then be disaggregated such that:

$$f_\ell(p_{\ell t}, q_{\ell t}) \leq w_{\ell t}, \quad \forall \ell \in \mathcal{L}, t \in \mathcal{T}, \tag{9}$$

[3]Note that if there is communication structure between multiple nodes, the DSO can issue a shared DOE (which will be a region in $\mathbb{R}^{2K}$ where $K$ is the number of consumers with communication) within each time interval and as long as they jointly keep their powers inside their DOE, the network's security is guaranteed.

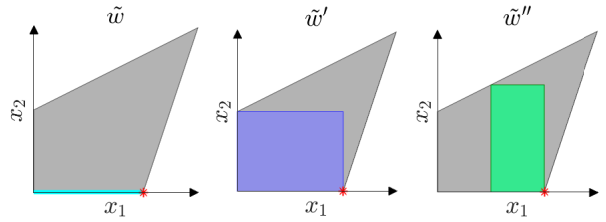


Figure 3. Different disaggregated feasible regions obtained using different sets of weights, where all of them contain the optimal solution of the problem (shown by red asterisk).

Note that constraint (9) for each consumer is independent of other consumers and given $w_{\ell t}$, leads to a two-dimensional feasible region $\mathbf{\Omega}_{\ell t}$:

$$\mathbf{\Omega}_{\ell t}(w_{\ell t}) := \{p_{\ell t}, q_{\ell t} \mid f_\ell(p_{\ell t}, q_{\ell t}) \leq w_{\ell t}\}, \quad \forall \ell \in \mathcal{L}, t \in \mathcal{T}. \tag{10}$$

Using the disaggregated feasible regions (10), the network optimisation model (4) can be updated to:

$$\min_{\mathbf{\Omega}(w)} \ \mathbb{C}^{net}(\mathbf{p}, \mathbf{q}) \tag{11}$$

where $\mathbf{\Omega}(w) : \mathbf{\Omega}_{11}(w_{11}) \times \cdots \times \mathbf{\Omega}_{LT}(w_{LT}) \subseteq \Xi_{\mathcal{N}}$ denotes the network's disaggregated feasible set. Let us denote the output of this disaggregated network problem by $\mathbf{\Omega}^\star(w) : \mathbf{\Omega}^\star_{11}(w_{11}) \times \cdots \times \mathbf{\Omega}^\star_{LT}(w_{LT})$.

For most networks, there will be an infinite number of possible ways to come up with a valid set of portions $w_{\ell t}$ such that (7) holds. To illustrate, an example of such setting for a system with two variables is shown in Fig. 3. The gray area shows the feasible region of the original problem with the optimal point shown with red star. The three disaggregated regions are obtained using three different set of portions $\tilde{w}$, $\tilde{w}'$ and $\tilde{w}''$ while all including the optimal point of the original problem.

In the following section, we explain how to systematically obtain the optimal set of portions.

### *E. Optimal Set of Portions $w^\star$*

Let us define $\mathcal{W}$ to denote the set of all such portions in order that $\mathbf{\Omega}_{\ell t}(w_{\ell t})$ is nonempty:

$$\mathcal{W} := \Big\{ w \in \mathbb{R}^{m \times L \times T}, w := [w_{\ell t}], \forall \ell \in \mathcal{L}, t \in \mathcal{T} \mid \sum_{\ell=1}^{L} w_{\ell t} = b_t, \forall t \in \mathcal{T} \ , \ f_\ell(p_{\ell t}, q_{\ell t}) \leq w_{\ell t}, \forall \ell \in \mathcal{L}, t \in \mathcal{T} \Big\}, \tag{12}$$

and subsequently, $\forall \tilde{w} \in \mathcal{W}$, the disaggregated network problem (11) can be re-expressed as:

$$\forall \tilde{w} \in \mathcal{W}, \ \exists \{ p^\star_{\ell t}, q^\star_{\ell t}, \forall \ell \in \mathcal{L}, t \in \mathcal{T} \} = \arg\min_{\mathbf{\Omega}(\tilde{w})} \mathbb{C}^{net}(\mathbf{p}, \mathbf{q}) \tag{13}$$

Let us denote this solution point by $\mathbf{\Omega}^\star(\tilde{w})$[4]. Also, let us assume that the problem (4) is convex and separable (we will return to these assumptions shortly), we can use Theorem 3.1 in [22] to show that, for each $\tilde{w} \in \mathcal{W}$, the optimal solution of the network disaggregated model (13) is also an optimal solution of (4), that is, $\forall \tilde{w} \in \mathcal{W}, \mathbf{\Omega}^\star(\tilde{w}) \in \Xi^*_{\mathcal{N}}$. In other words, our disaggregated model (13) preserves the optimal solution of the original network model (4).

As mentioned in Section III-D, the network and the consumers do not always have the same objective. However, if their objectives coincide, the central problem (3) will have the same objective as the network problem (4). This enables us to preserve the optimal solution to (3) using our disaggregated model. In Section IV-A, we will present examples of each of these cases. Later, in Section V, we will investigate the impact of having the same versus different objectives for the network and consumers on the solution quality of our disaggregation approach.

**Remark:** A function $f : \mathbb{R}^n \to \mathbb{R}$ is said to be separable if it can be expressed as a sum of functions that depend only on a subset of the variables. Specifically, a function $f$ is separable if there exist functions $f_1, f_2, \ldots, f_n$ such that

$$f(x_1, x_2, \ldots, x_n) = \sum_{i=1}^{n} f_i(x_i),$$

where $x_i \in \mathbb{R}$ for $i = 1, 2, \ldots, n$. Intuitively, a separable function is one that can be broken down into simpler functions that depend only on one or a few variables, rather than all of them [25]. In Section IV-A, we demonstrate that the constraints in the network problem (4) can be reformulated as separable and convex functions of each consumer's real and reactive power injection.

Solving the optimisation model (11) will provide an acceptable set of portions. However, one should note that there might exist other sets of portions which result in the same optimal solution, i.e., $\exists \tilde{w}, \tilde{w}', \ \mathbf{\Omega}^\star(\tilde{w}) = \mathbf{\Omega}^\star(\tilde{w}')$. It is important to notice this as different sets of portions lead to different DOEs for consumers while still preserving the optimal solution of the network.

To determine an optimal set of portions, denoted by $w^\star$, we first identify an objective characterised by a function $g(w)$ and update the disaggregated network problem (11) to:

$$\min_{\mathbf{\Omega}(\tilde{w}) \cap \mathcal{W}} \ \mathbb{C}^{net}(\mathbf{p}, \mathbf{q}) + \varepsilon g(w), \tag{14}$$

where the second term in objective, i.e., $\varepsilon g(w)$, with $\varepsilon$ being a very small parameter, is a regularisation term and it enables our model to select an optimal set of portions $w^\star$ among all the acceptable set of portions denoted by $\mathcal{W}$ while not harming the primary objective (first term in objective). The output of this optimisation is $\mathbf{\Omega}^\star(w^\star) : \mathbf{\Omega}^\star_{11}(w^\star_{11}) \times \cdots \times \mathbf{\Omega}^\star_{LT}(w^\star_{LT})$.

To identify the function $g(w)$, we first introduce an index called *Contribution Index* for each consumer within each time interval, which represents the total contribution of this consumer to satisfy all the network's constraints within time interval $t$. We represent the Contribution Index for consumer $\ell$ at time $t$ as a vector $C_{\ell t}$, whose elements are obtained as:

$$C_{\ell t,h} := \frac{w_{\ell t,h}}{b_{t,h}} \tag{15}$$

[4]Note that each element in $\mathbf{\Omega}^\star(\tilde{w})$, e.g., for time-step $t$ and consumer $\ell$, $\mathbf{\Omega}^\star_{\ell t}(\tilde{w}_{\ell t})$ whose definition is shown in (10) represents a polygon bounded by $m$ straight sides denoted by $f_\ell(p_{\ell t}, q_{\ell t}) \leq \tilde{w}_{\ell t}$. We refer to this polygon as a two-dimensional envelope in a $(p_{\ell t}, q_{\ell t})$ plane. Examples of such polygons are shown in Section V.

where $C_{\ell t,h}$ is the contribution of consumer $\ell$ in satisfying the $h$-th network's constraint within time interval $t$. This contribution is defined as the percentage of this consumer's portion $w_{\ell t,h}$ from the total right-hand side corresponding to $h$-th constraint, i.e., $b_{t,h}$. Let us collect all the contribution indices in a vector $C = [C_{\ell t}^{\intercal} \quad \forall \ell \in \mathcal{L}, t \in \mathcal{T}]^{\intercal}$. We then utilise this index to investigate two different objective functions:

- *Close-to-Equal Contributions*: this objective function minimises the standard deviation of consumers' contributions from equal contribution. Based on this objective, the set of portions which results in close-to-equal contribution indices for all consumers is desirable. This function is defined using:

$$g_1(w) := \left\| C - \overline{C} \right\| \tag{16}$$

  where vector $\overline{C} = [\frac{1}{L}, ..., \frac{1}{L}]$ denotes the equal contribution index.
- *Contributions Relative to Inverse Sensitivities*: under this objective, each consumer contributes relative to their sensitivities to each network constraint. This objective is defined:

$$g_2(w) := \| C - S \| \tag{17}$$

  where $S$ is a vector describing the inverse relative sensitivity of nodal voltage magnitudes and line powers to the consumers' real power injection. Specifically, $S$ collects the sensitivities of all consumers' and at all time steps and is defined as $S := [S_{\ell t}^{\intercal} \quad \forall \ell \in \mathcal{L}, t \in \mathcal{T}]^{\intercal}$. We consider $S_{\ell t} = [SV_{\ell t}^{\intercal}, SP_{\ell t}^{\intercal}]^{\intercal}$, where vectors $SV_{\ell t}$ and $SP_{\ell t}$ denote the inverse sensitivity of nodal voltage magnitudes and line powers to the real power injection of consumer $\ell$ and time $t$, respectively. The elements in $SV_{\ell t}$ and $SP_{\ell t}$ are obtained as follows:

$$SV_{\ell t}^{i\phi} = (\frac{\partial V_{i\phi t}}{\partial p_{\ell t}})^{-1}, \quad SP_{\ell t}^{ij\varphi t} = (\frac{\partial S_{ij\varphi t}}{\partial p_{\ell t}})^{-1} \tag{18}$$

  where $\frac{\partial V_{i\phi t}}{\partial p_{\ell t}}$ denotes the sensitivity of the voltage magnitude at node $(i\phi)$ and time $t$ to the real power injection of consumer $\ell$ at time $t$. Also, $\frac{\partial S_{ij\varphi t}}{\partial p_{\ell t}}$ denotes the sensitivity of the line power at line $(i, j)$ and phase $\varphi$ during time $t$ to the real power injection of consumer $\ell$ at time $t$.

Based on the selected objective function, $g_1(w)$ or $g_2(w)$, we solve the disaggregated network problem (14) which outputs the optimal set of portions $w^{\star}$ and accordingly we can determine the DOE of each consumer, i.e., $\mathbf{\Omega}_{\ell t}(w^{\star}), \forall \ell \in \mathcal{L}, t \in \mathcal{T}$ using (10). These DOEs will then be sent to each consumer.

### F. Consumer Problem

Each consumer receives its DOEs[5], i.e., $\mathbf{\Omega}_{\ell t}, \forall t \in \mathcal{T}$, which can be in the basis of day-ahead or year-ahead based on the application, from the network. Each consumer requires to integrate its DOEs as constraints in their scheduling and / or planning. For DER capacity assessment, each consumer $\ell$ solves an optimisation problem given by:

$$\min_{\Xi_\ell} \ \mathbb{C}_\ell(\boldsymbol{x}_\ell) \tag{19a}$$

$$(1) \tag{19b}$$

$$\Xi_\ell := \left\{ \boldsymbol{x}_\ell := [G_\ell^{der}, p_{\ell t}^{der}, q_{\ell t}^{der}], \forall t \in \mathcal{T} \mid k_\ell(\boldsymbol{x}_\ell) \leq e_\ell \right\} \cap \mathbf{\Omega}_{\ell t}, \tag{19c}$$

which optimises their DER size and operation based on their objective function $\mathbb{C}_\ell$, such that *i)* the consumer's connection point powers stay inside its DOE, and *ii)* the DER's operational constraints (e.g. inverter's constraints) are respected. The latter constraints are represented by vector function $k_\ell$ and vector parameter $e_\ell$. Using the optimisation model (19), which entails the corresponding node's DOE as a constraint, the consumer can make the planning (e.g. size of the installed PV system and battery storage systems) and operation decisions (e.g. PV real power curtailment and battery storage real power charging and discharging decisions) in order to optimally use the network's capacity that has been assigned to it through its DOE.

## IV. Detailed DER Capacity Assessment Model

In this section, we detail the network's and consumers' constraints, i.e., constraints $f(\mathbf{p}, \mathbf{q}) \leq \mathbf{b}$ and $k_\ell(\boldsymbol{x}_\ell) \leq e_\ell$ in (4b) and (19c), for DER capacity assessment problem.

### A. Network Problem: Extended Form

We model the physics of the network using the linear power flow model used in [26] as given below:

$$\mathbf{U} = \mathbf{1}U_0 + \tilde{\mathbf{R}}\mathbf{p} + \tilde{\mathbf{X}}\mathbf{q} \tag{20}$$

where $\mathbf{U} := |\mathbf{V}|^2$ is the vector of nodal squared voltage magnitudes, $\mathbf{p}$ and $\mathbf{q}$ are vectors of net nodal real and reactive power injections, $\mathbf{1}$ is a vector of all ones and $U_0 = |V_0|^2$ is the squared voltage magnitude of the slack node. $\tilde{\mathbf{R}}$ and $\tilde{\mathbf{X}}$ are sensitivity matrices under no-load condition such that:

$$\tilde{R}_{j,\varphi}^{i,\phi} = \frac{\partial U_{i\phi}}{\partial p_{j\varphi}} \quad , \quad \tilde{X}_{j,\varphi}^{i,\phi} = \frac{\partial U_{i\phi}}{\partial q_{j\varphi}} \tag{21}$$

where $\tilde{R}_{j,\varphi}^{i,\phi}$ and $\tilde{X}_{j,\varphi}^{i,\phi}$ respectively represent the sensitivity of squared voltage magnitude of node $i$ and phase $\phi$ to the net injected real and reactive power of node $j$ and phase $\varphi$. The accuracy of the linear power flow model (20) is comprehensively studied in [27], [28]. These studies demonstrate that the linear model can reliably approximate voltage magnitudes with less than 0.5% error across a wide range of scenarios and different problem types. It is important to note that we only use the linear power flow model in our optimisation framework. However, when calculating real-time voltage magnitudes to assess the number of voltage violations, we employ an exact full-AC power flow model. Furthermore, in addition to the voltage and thermal limits that we have incorporated into our network operational constraints, other constraints such as limiting the voltage unbalanced factor can be similarly incorporated into our optimal power flow problem [29].

We then define the following sets of constraints in the network problem:

[5]Note that our assumption in the network problem, i.e., when calculating the DOEs, is that the consumers will adhere to their assigned DOEs in the real-time operation. Thus, how many and what kind of devices are installed behind the meter will not impact the networks' safety as long as the consumers act within their envelopes. We left assessing the risk of some consumers not being able to respect their DOEs to future work.

*1) Voltage Constraints:* Using power flow model (20), the voltage magnitude constraint $\forall i \in \mathcal{V}, \phi \in \Phi, t \in \mathcal{T}$ is written:

$$\underline{U} \leq U_0 + \sum_{(j,\varphi)\in\mathcal{V}_g} (\tilde{R}^{i,\phi}_{j,\varphi} p_{j\varphi t} + \tilde{X}^{i,\phi}_{j,\varphi} q_{j\varphi t}) \leq \overline{U} \tag{22}$$

where $\underline{U}$ and $\overline{U}$ are square of acceptable lower and upper voltage bounds.

*2) Branch Thermal Constraints:* The branch thermal constraints specify the maximum real and reactive power that can flow through each line and $\forall ij \in \mathcal{E}, \varphi \in \Phi, t \in \mathcal{T}$ is written:

$$P^2_{ij,\varphi t} + Q^2_{ij,\varphi t} \leq \overline{S}^2_{ij,\varphi} \tag{23}$$

where $\overline{S}_{ij,\varphi}$ denotes the maximum allowed apparent power for the corresponding branch. This is a quadratic constraint and represents the inner area of a circle in $(P_{ij,\varphi t}, Q_{ij,\varphi t})$ coordinates. This constraint can be approximated with $2\rho$ affine constraints where $\rho \geq 2$ is an arbitrary integer number [30]. These affine constraints are:

$$(\cos\theta - \sin\theta)P_{ij,\varphi t} + (\cos\theta + \sin\theta)Q_{ij,\varphi t} \leq \sqrt{2}\,\overline{S}_{ij,\varphi}, \tag{24}$$

where $\theta \in \Theta := \{0, \pi/\rho, 2\pi/\rho, ..., (2\rho-1)\pi/\rho\}$.

When using power flow model (20), power flows of each branch $(i,j)$ and phase $\varphi$ can be replaced with the total net nodal consumption (negative injection) of all the nodes downstream (further from the slack node) of the node $j$ and phase $\varphi$, including itself, where we denote them with the set $\mathcal{D}_{j\varphi}$. With this in mind, the branch thermal limits are re-expressed as:

$$\begin{aligned}(\cos\theta - \sin\theta) \sum_{(k,\varphi)\in\mathcal{D}_{j\varphi}} (-p_{k\varphi t}) + (\cos\theta + \sin\theta) \sum_{(k,\varphi)\in\mathcal{D}_{j\varphi}} (-q_{k\varphi t}) \\ \leq \sqrt{2}\,\overline{S}_{ij,\varphi}, \quad \forall ij \in \mathcal{E}, \varphi \in \Phi, t \in \mathcal{T}, \theta \in \Theta\end{aligned} \tag{25}$$

*3) Consumer Preferences and Operation Considerations:* When calculating the DOEs for the participant consumers, the real and reactive power of the non-participate consumers are fixed as follows:

$$p_{j\varphi t} = -p^d_{j\varphi t},\ q_{j\varphi t} = -q^d_{j\varphi t} \quad \forall (j,\phi) \in \mathcal{V}_{g'},\ t \in \mathcal{T} \tag{26}$$

where the parameters $p^d_{j\varphi t}$ and $q^d_{j\varphi t}$ are forecasted using the consumers' historical data. Also, the real power of the participant consumers are constrained by:

$$\underline{p}_{j\varphi t} \leq p_{j\varphi t} \leq \overline{p}_{j\varphi t} \quad \forall (j,\phi) \in \mathcal{V}_g,\ t \in \mathcal{T} \tag{27}$$

where the parameters $\underline{p}_{j\varphi t}$ and $\overline{p}_{j\varphi t}$ denote the allowable lower and upper bounds of the net real power injection of the corresponding node within time interval $t$. These bounds can be selected either by DSO or each consumer (based on their preferences). Therefore, we write:

$$\underline{p}_{j\varphi t} := \max(\underline{p}^{cstm}_{j\varphi t}, \underline{p}^{dso}_{j\varphi t}) \quad , \overline{p}_{j\varphi t} := \min(\overline{p}^{cstm}_{j\varphi t}, \overline{p}^{dso}_{j\varphi t}) \tag{28}$$

where $\underline{p}^{cstm}_{j\varphi t}$ and $\overline{p}^{cstm}_{j\varphi t}$ denote the desired lower and upper bounds of the consumer that can be periodically sent to the DSO. These bounds sent by each consumer can empower the DSO to make more informed decisions and better utilise the network's capacity. Also, $\underline{p}^{dso}_{j\varphi t}$ and $\overline{p}^{dso}_{j\varphi t}$ are the bounds defined by the DSO which are typically considered for two reasons: $i$) the upper bound is to avoid unrealistically large injections, especially for the consumers in a close proximity of the substation as the network's constraints are less sensitive to power injections of these consumers, and $ii$) the lower bound is to provide an opportunity for all consumers to access/utilise the network's capacity. These bounds can be determined using the forecast or historical data[6].

In summary, we formulate the network problem as a linear programming optimisation problem, subject to the following constraints: (21), (22), (25), (26), (27) and (28), with the objective (4a). We solve this optimisation problem using the Gurobi solver [32] in our experiments.

### *B. Consumer Problem: Extended Form*

Without loss of generality, we assume that the participant consumers are interested in installing PV and battery storage systems, although our consumer modelling approach in Section III can accommodate other DER systems as well. To this end, we propose the following optimisation model. For each participant consumer $\ell$, we define $C^{planning}_\ell$ and $C^{operation}_\ell$ as the investment capital cost of purchasing DER systems and their operation, respectively. Let $C^{pv}_\ell$ and $C^{batt}_\ell$ denote the cost of buying PV and battery storage systems. Let $C^{buy}_{\ell t}$ and $C^{sell}_{\ell t}$ denote price of buying and selling power from and to the grid at time $t$. Let $p^{buy}_{\ell t}$ and $p^{sell}_{\ell t}$ be the bought and sold power from and to the grid from consumer $\ell$ at time $t$. Also, let $p^{batt}_{\ell t}$, $q^{batt}_{\ell t}$, $p^{pv}_{\ell t}$ and $q^{pv}_{\ell t}$ denote the real and reactive power injection of the battery storage and PV systems at time $t$. To evaluate the effectiveness of our right-hand-side allocation technique in maintaining the optimal solution, we analyse two different objective functions for consumers. The first objective minimises the overall cost of installing and operating DER units, while the second objective aims to maximise the amount of consumer real power throughput to the grid, similar to the network's objective function. These objectives are formulated $\forall \ell \in \mathcal{L}$ as follows:

- *Cost minimisation*

$$\min \quad C^{planning}_\ell + C^{operation}_\ell \tag{29a}$$
$$C^{planning}_\ell = C^{batt}_\ell + C^{pv}_\ell \tag{29b}$$
$$C^{operation}_\ell = \sum_{t\in\mathcal{T}} C^{buy}_{\ell t} p^{buy}_{\ell t} - C^{sell}_{\ell t} p^{sell}_{\ell t} \tag{29c}$$
$$p^{sell}_{\ell t} - p^{buy}_{\ell t} = p^{batt}_{\ell t} + p^{pv}_{\ell t} - p^d_{\ell t} \tag{29d}$$
$$q_{\ell t} = -q^d_{\ell t} + q^{batt}_{\ell t} + q^{pv}_{\ell t} \tag{29e}$$
$$\left(p^{sell}_{\ell t} - p^{buy}_{\ell t}, q_{\ell t}\right) \in \mathbf{\Omega}_{\ell t} \tag{29f}$$

[6]Note that although we consider a radial power flow model to test our DOE approach, our modelling is general and can also be used to power systems. As discussed in Section III-E, our approach requires the constraints to be convex and only include separable functions. Therefore, we can apply the linear power flow model from [31] to formulate an optimal power flow problem for meshed distribution networks.

- *Real power throughput maximisation:*

$$\max \sum_{t\in\mathcal{T}} p_{\ell t} \tag{30a}$$

$$p_{\ell t} = p^{batt}_{\ell t} + p^{pv}_{\ell t} - p^{d}_{\ell t} \tag{30b}$$

$$q_{\ell t} = -q^{d}_{\ell t} + q^{batt}_{\ell t} + q^{pv}_{\ell t} \tag{30c}$$

$$\big(p_{\ell t}, q_{\ell t}\big) \in \mathbf{\Omega}_{\ell t} \tag{30d}$$

In the following, we define the PV and battery storage system operational constraints, separately. These constraints are then added to the above optimisation problems.

*1) PV System Constraints:* For each consumer $\ell$, let $p^{g}_{\ell t}$ and $p^{cur}_{\ell t}$ denote the available real power for generation and the real power curtailment of the PV system at time $t$. Let $G^{pv}_{\ell}$ denote the PV installed capacity. Also, parameter $\eta_t \in [0,1]$ denotes the efficiency coefficient of PV panels, which is defined as the ratio of actual power generated by PV to its installed capacity and is a function of environmental factors including solar irradiance and temperature. We then consider the following model for the PV systems:

$$p^{pv}_{\ell t} = p^{g}_{\ell t} - p^{cur}_{\ell t}, \quad p^{g}_{\ell t} = \eta_t G^{pv}_{\ell} \tag{31}$$

$$0 \le p^{cur}_{\ell t} \le p^{g}_{\ell t} \tag{32}$$

$$(\cos\vartheta - \sin\vartheta)p^{pv}_{\ell t} + (\cos\vartheta + \sin\vartheta)q^{pv}_{\ell t} \le \sqrt{2}G^{pv}_{\ell} \tag{33}$$

$$C^{pv}_{\ell} = \gamma^{pv} G^{pv}_{\ell} \tag{34}$$

where $\vartheta \in \Theta := \{0, \pi/\rho, 2\pi/\rho, ..., (2\rho-1)\pi/\rho\}$. Constraint (32) enforces the real power curtailment of the PV system to be positive and no more than PV's available real power for generation. Constraint (33) denotes the linearised PV inverter's thermal limit, which is derived similarly to the linearisation of line thermal limits in (25) (note that we assume the PV inverter size is the same as the installed PV panel size). Additionally, constraint (34) assumes a linear relationship between the price of a PV system and its capacity[7].

*2) Battery Storage System Constraints:* For each consumer $\ell$, let $p^{ch}_{\ell t}$, $p^{dis}_{\ell t}$ and $E^{batt}_{\ell t}$ denote the real power charge and discharge, and the state-of-charge of the battery at time $t$. Also, let $\overline{p}^{ch}_{\ell}$, $\overline{p}^{dis}_{\ell}$ and $\overline{E}^{batt}_{\ell}$ denote the maximum real power charge and discharge rates, and the maximum state-of-charge of the battery. In addition, let $\delta$ denote the duration of each time interval. Consider the binary variable $u_{\ell t} \in 0, 1$, where the value 1 indicates that the battery is charging and the value 0 indicates that the battery is discharging. Let $G^{batt}_{\ell}$ be the battery inverter size. Let $\gamma^{batt}\mathcal{R}$ denote the relation between the battery price and its specification, with $\gamma^{batt}$ being a constant. Additionally, let parameter $\eta^{batt}_{\ell}$ denote the battery round-trip efficiency.

$$p^{batt}_{\ell t} = p^{dis}_{\ell t} - p^{ch}_{\ell t} \tag{35a}$$

$$E^{batt}_{\ell t} = E^{batt}_{\ell,t-1} + \delta(\eta^{batt}_{\ell} p^{ch}_{\ell t} - \frac{p^{dis}_{\ell t}}{\eta^{batt}_{\ell}}) \tag{35b}$$

$$0 \le p^{dis}_{\ell t} \le \overline{p}^{dis}_{\ell},\ 0 \le p^{ch}_{\ell t} \le \overline{p}^{ch}_{\ell},\ 0 \le E^{batt}_{\ell t} \le \overline{E}^{batt}_{\ell} \tag{35c}$$

$$p^{ch}_{\ell t} \le \mathcal{M} u_{\ell t}, \quad p^{dis}_{\ell t} \le \mathcal{M}(1 - u_{\ell t}) \tag{35d}$$

$$(\cos\vartheta - \sin\vartheta)p^{batt}_{\ell t} + (\cos\vartheta + \sin\vartheta)q^{batt}_{\ell t} \le \sqrt{2}G^{batt}_{\ell} \tag{35e}$$

$$C^{batt}_{\ell} = \gamma^{batt}\mathcal{R}, \quad \mathcal{R} = \overline{p}^{ch}_{\ell} = \overline{p}^{dis}_{\ell} = \frac{\overline{E}^{batt}_{\ell}}{\delta} = G^{batt}_{\ell} \tag{35f}$$

[7]While we assume a linear relationship between the price of a PV system and its capacity for simplicity, it is worth noting that other convex functions can also be used to model the price.

*3) Uncertainty Modelling (Box Uncertainty Set and Adjustable Robust Formulation):* For each participant consumer $\ell$, the real power demand $p^{d}_{\ell t}$ and PV efficiency coefficient $\eta_t$ are uncertain parameters. In our modelling, we consider that these uncertain parameters belong to the following polyhedral uncertainty sets:

$$\mathcal{U}_d := \{p^{d}_{\ell t} \in \mathbb{R} \mid p^{d}_{\ell t} = \hat{p}^{d}_{\ell t} + \Delta p^{d}_{\ell t}, \ \underline{\Delta p}^{d}_{\ell t} \le \Delta p^{d}_{\ell t} \le \overline{\Delta p}^{d}_{\ell t}\} \tag{36}$$

$$\mathcal{U}_{pv} := \{\eta_t \mid 0 \le \hat{\eta}_t + \Delta\eta_t \le 1\ ,\ \underline{\Delta\eta}_t \le \Delta\eta_t \le \overline{\Delta\eta}_t\} \tag{37}$$

where random variables $\Delta p^{d}_{\ell t}, \Delta\eta_t \in \mathbb{R}$ denote demand and PV efficiency coefficient fluctuations from their forecasted values $\hat{p}^{d}_{\ell t}$ and $\hat{\eta}_t$. These fluctuations are bounded between given lower and upper bounds.

To account for the uncertainties in our optimisation problem and ensure that the constraints hold for any possible realisations of the uncertain parameters within their defined uncertainty set, we adopt a robust optimisation framework. In particular, we employ the affinely adjustable robust counterpart (AARC) methodology to model the fast-responding capabilities of batteries and inverters for taking corrective actions once uncertainties are realised. To implement the AARC methodology, we define the following affine policies:

$$\boldsymbol{x}_{\ell t}(\Delta\eta_t, \Delta p^{d}_{\ell t}) := \boldsymbol{x}^{0}_{\ell t} + \boldsymbol{\alpha}^{pv}_{\ell t}\Delta\eta_t + \boldsymbol{\alpha}^{d}_{\ell t}\Delta p^{d}_{\ell t} \tag{38}$$

Here, $\boldsymbol{x}_{\ell t} = [p^{cur}_{\ell t}, q^{pv}_{\ell t}, p^{ch}_{\ell t}, p^{dis}_{\ell t}, q^{batt}_{\ell t}]^{\intercal}$ are the variables associated with fast-acting devices. In the AARC methodology, we treat $\boldsymbol{x}^{0}_{\ell t}$, $\boldsymbol{\alpha}^{pv}_{\ell t}$, and $\boldsymbol{\alpha}^{d}_{\ell t}$ as decision variables, which we obtain by solving the consumer optimisation problem. During real-time operation, they become fixed and serve as parameters for the affine functions. In the Appendix section, we have provided the detailed reformulation of the consumer problem using the AARC methodology. Also, For more information on using AARC in power system optimisation problems, please refer to [28] and [33].

## V. Numerical Results and Discussion

In this section, we assess the DER capacity of two unbalanced distribution systems, including the IEEE 906-node LV system and the IEEE 37-node MV system. We specifically selected these networks to validate our proposed approach on both voltage-constrained (IEEE 906-node) and thermally-constrained (IEEE 37-node) networks. We first examine our proposed DOE-based approach under the two discussed regularisation terms, resulting in different objective functions, and compare their results with the central case. We then benchmark our approach against the available methods in the literature, including fixed and dynamic export limits. Before presenting our numerical results, we briefly summarise our proposed modelling and experiment setup in the following section.

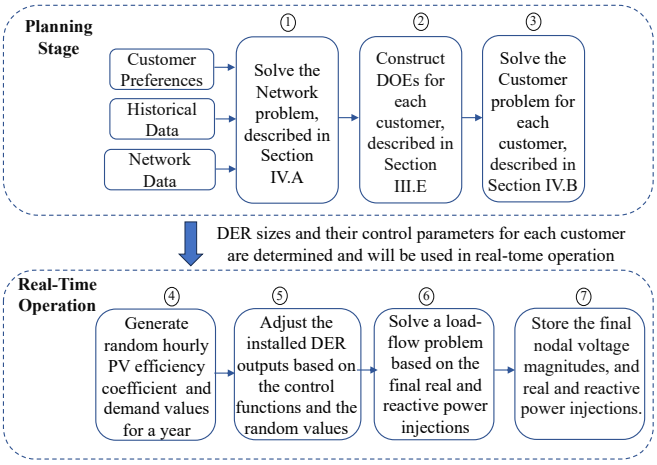


Figure 4. An overview of the proposed method and the numerical experiment setup.

### A. Overview of the Proposed Method and the Experiment Setup

Figure 4 provides an overview of our approach at the top level. ①: We begin by collecting consumer preferences, historical data, and network data. We then solve the network optimisation problem described in Section IV-A to obtain the optimal set of network partitions, denoted as $w^{\star}$. ②: For each consumer and time step, we construct a two-dimensional DOE based on (10). ③: The consumer problem, discussed in Section IV-B, is subsequently solved to determine the planning decisions. These decisions include selecting appropriate sizes for batteries and inverters, as well as determining the parameters of the controller function described in (38).

The bottom level of Fig. 4 outlines our numerical experiment setup. To assess the performance of our proposed approach in real-time operation, we introduce random hourly scenarios, which account for the stochastic variations in both PV generation and demand from their predicted value. ⑤: Utilising these randomly generated scenarios as input for the function (38), we calculate real-time values for PV inverter generation (both real and reactive power) and battery charging and discharging (real and reactive power injections) for each node. In step ⑥, we employ the nodal real and reactive power injections to solve a load flow problem using the full-AC power flow model. Finally, in step ⑦, we store the nodal voltage magnitudes and line currents obtained from step ⑥, along with the consumers' behind-the-meter information acquired from steps ④ and ⑤.

### B. Simulation Data

In our simulations, the voltage of slack node is fixed at 1.0 per unit (pu) and the acceptable voltage limits are considered in [0.95,1.05] pu. The thermal limit of the transformer is utilised for both branches and transformer[8]. This thermal limit is 800 kVA for the IEEE 906-node system and 2.5 MVA for the IEEE 37-node. We use the demand and PV generation profile data with hourly resolution from [34], [35]. Also, the optimisation parameters for these experiments are summarised in Table. I. We consider that 25% of the consumers wish to participate in the planning trial. We also show how increasing the percentage of consumer participants will affect the DOEs. Our experiments also assume parameters $\underline{p}^{dso}_{j\varphi t}$ and $\overline{p}^{dso}_{j\varphi t}$ were set to $-250\%$ and $+250\%$ of each consumer's maximum yearly demand, respectively. We consider a time-of-use pricing scheme to calculate DER operation cost in (29) extracted from [36]. We also set $\varepsilon$ in (14) to 0.01 using an iterative trial and error approach and left using a more systematic approach to set this parameter for future work. The price of buying and selling electricity is extracted from [37]. Also, capital costs for PV and battery storage systems are obtained from [38] and [39], respectively.

Table I
MODEL PARAMETERS.

| **Parameter** | $\varepsilon$ | $\underline{p}^{cstm}_{j\varphi t}, \overline{p}^{cstm}_{j\varphi t}$ | $\underline{p}^{dso}_{j\varphi t}, \overline{p}^{dso}_{j\varphi t}$ |
|---|---|---|---|
| **Value** | 0.01 | $\hat{p}^{d}_{j\varphi t} + \overline{\Delta p}^{d}_{j\varphi t}$ , $+\infty$ | -2.5 $p^{d}_{max}$ , 2.5 $p^{d}_{max}$ |

Due to the constraints of conducting our experiments on a personal laptop, we have constrained our study horizon to one year, a practical choice that allowed us to comprehensively investigate essential parameters such as regularisation terms, customer participation percentages, and alternative approaches. Thus, we appropriately scale the capital investment costs to ensure a meaningful comparison between capital investments and operational expenses over our one-year planning period. Nevertheless, the potential for future research is substantial. Subsequent endeavours could broaden the scope of simulation results by considering a more extended study duration. This extension could also account for the inherent uncertainty linked to the costs of DERs and the dynamic nature of the electricity market, which would yield a more precise economic assessment of hosting capacity within distribution systems.

### C. DOE-Based DER Capacity Assessment Results

We solve the network problem at the first level of our proposed framework, once with the regularisation term (16), i.e., *Close-to-Equal Contributions*, and another with the regularisation term (17), i.e., *Contributions Relative to Inverse Sensitivities*. The output of the first level is the DOEs of each consumer during each time interval for the whole study horizon. Examples of DOEs for the IEEE 37-node test system, considering 25% of consumers participating in the experiment, are shown in Fig. 5. We have included DOEs of consumers located at different parts of the test feeder to show the implications of different regularisations on different consumers.

[8]We have set up our experiments based on the available data in the IEEE 37 and 906 test systems. Thus, since these datasets lack the thermal limit for each line and only provide the thermal limit for the transformers, we use the transformer's thermal limit for the branches as well. Please note that this is not a part of our proposed approach and is related to data.

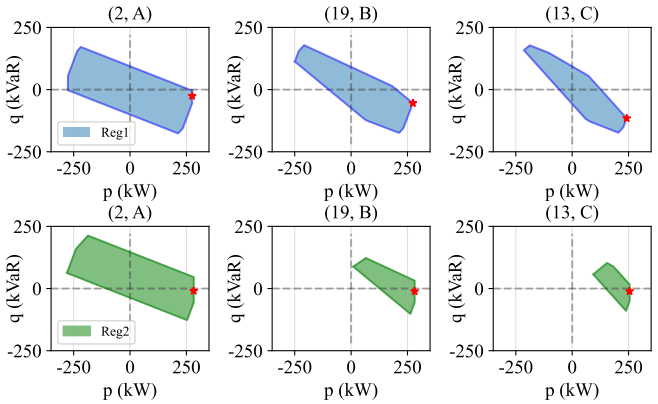


Figure 5. Examples of DOEs in IEEE 37-node MV system under 100% consumer participation. The top and bottom rows show the DOEs when using *Close-to-Equal Contributions* (Reg1) and *Contributions Relative to Inverse Sensitivities* (Reg2) regularisation terms, respectively.

Particularly, we have selected nodes (2,A), (19,B) and (13,C), which are located at the beginning, middle and end of the feeder in the 37-node system, respectively, to highlight the impact of variations in voltage sensitivities along the feeder on the DOEs. Based on the selected regularisation term, the DOEs can significantly change for a specific consumer (see the DOEs allocated to node (13,C) in Fig. 5) while the optimal solution, shown with a red star, of the network problem will still be preserved inside DOEs. Additionally, this figure demonstrates that employing the *Close-to-Equal Contributions* regularisation term results in more uniformly allocated regions for different nodes in the grid. This finding suggests the possibility of achieving more equitable operating envelopes for diverse consumers while effectively utilising the full network capacity to accommodate additional DERs. This is evident in the first row of this figure, showing DOEs that are relatively closer to each other for different nodes under the *Close-to-Equal Contributions* regularisation term, compared to the second row that shows the alternative.

Our approach empowers consumers by allowing them the freedom to install any DER of their choice and determine its capacity based on their preferences. However, to ensure fair allocation of network capacity among consumers, we adopt a methodology that limits the maximum network access for each consumer rather than restricting the capacity of individual DERs. This means consumers can still install DERs of any size as long as their grid injection and absorption remain within their allocated DOEs. Limiting the maximum network access prevents the optimisation process from allocating all the capacity to a single node, leaving other nodes with no access. In LV systems, consumers typically do not require such large network access. Allocating all network capacity to a single node would be an inefficient use of network capacity and unfair to consumers connected to other nodes. Nevertheless, more studies are required to explore the impact of operating envelopes on distribution systems' fair and equitable operation.

Fig. 6 demonstrates that the DOE assigned to a consumer can vary across time steps. These temporal variations stem from alterations in the network's operating conditions, such

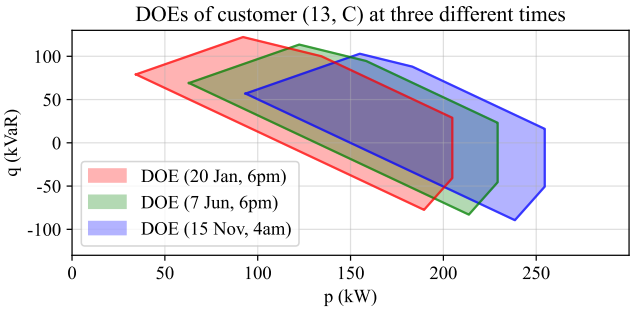


Figure 6. DOEs of the consumer located at node (13, C) during three different time steps in the IEEE 37-node test system.

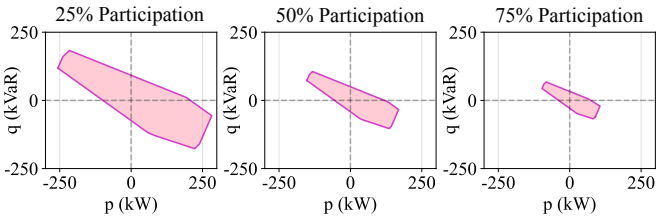


Figure 7. DOE of the consumer located at node (19, B) under three different consumer participation in the IEEE 37-node test system.

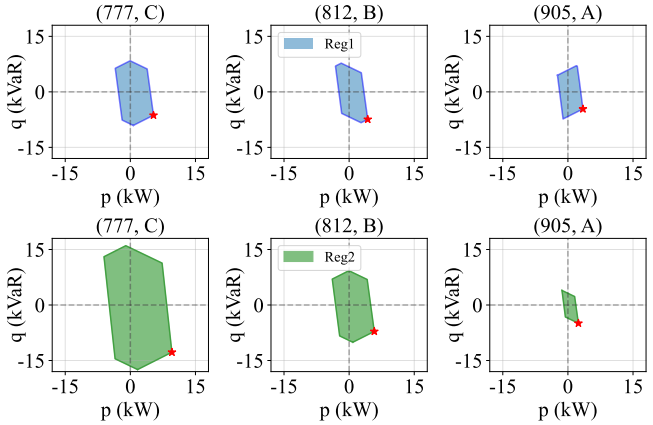


Figure 8. Examples of DOEs in IEEE 906-node LV system under 100% consumer participation. The top and bottom rows show the DOEs when using *Close-to-Equal Contributions* (Reg1) and *Contributions Relative to Inverse Sensitivities* (Reg2) regularisation terms, respectively.

as variations in the demand of non-participating consumers. Additionally, as illustrated in Fig. 7, increasing the percentage of consumer participation results in reduced DOEs for each participant. This effect occurs because our approach distributes the remaining network capacity amongst the participating consumers, resulting in a decrease in the share of the network capacity allocated to each consumer as the number of participating consumers increases. Furthermore, Fig. 8 presents examples of DOEs for the IEEE 906-node test system, similar to the 37-node system, for the 25% consumer participation and three nodes at the beginning, middle and end of the feeder. Comparing the DOEs in the 37-node and 906-node system, we can see that as the network size and the electrical distance between consumer nodes increases, the DOEs shrink.

Table II
SUMMARY OF THE OUT-OF-SAMPLE SIMULATION RESULTS IN THE IEEE 37-NODE NETWORK.

| Approach / Objective | | Maximum Export (MWh) | Minimum Cost ($) |
|---|---|---|---|
| Central | | 18397.8 | -3847200 |
| Proposed | Reg 1 | 18397.8 | -3751600 |
| | Reg 2 | 18397.8 | -3729800 |

Table III
SUMMARY OF THE OUT-OF-SAMPLE SIMULATION RESULTS IN THE IEEE 906-NODE NETWORK

| Approach / Objective | | Maximum Export (MWh) | Minimum Cost ($) |
|---|---|---|---|
| Central | | 1689.3 | -25084 |
| Proposed | Reg 1 | 1689.3 | -24153 |
| | Reg 2 | 1689.3 | -23944 |

At the second level of our framework, consumers use the received DOEs from the network as constraints in their optimisation model to determine the optimal installation capacity for their PV and battery storage systems, as well as the affine control functions required to adjust their DERs in real time. We evaluate the effectiveness of our proposed approaches using parameters obtained from the consumers' optimisation models. To test the out-of-sample performance, we generate 1000 scenarios for each time step, assuming that the stochastic variations of PV generations and demand follow a Beta distribution (with parameters extracted from [40]) and Normal distribution, respectively. We model the PV power and demand within a polyhedral uncertainty set in a robust optimisation framework. Therefore, the optimisation problem is independent of the data distribution as we only work with an uncertainty set box that can include any distribution. However, to be able to show the performance of our approach for a large number of scenarios, we have used the Beta and Normal distributions to generate the scenarios[9]. The simulation results are summarised in Tables II and III. Our results demonstrate that for the case of maximum real power throughput, the disaggregated approaches achieved the same solution as the central approach, consistent with the discussion in Section III-E about preserving optimal solution when the network and consumers share the same objective. For the other objective, our disaggregation approaches performed close to the central approach, with a decrease in the cost of only 2.5% and 3.1% for the IEEE 37-node system and 3.7% and 4.5% for the IEEE 906-node system compared to the central approach, respectively.

### *D. Comparison with Alternative DOE-Based Approaches*

In this section, we compare our proposed approach with other DOE-based methods, including 1) fixed real power export limit (FEL), i.e., 5 kW as used in [41], 2) optimal power flow based fixed real power export (OFEL) limit, as suggested by [42], and 3) dynamic real power export limit (DEL) calculated on an hourly basis, as suggested by [19]. In order to ensure a fair comparison, we exclude the reactive power component from our approach since none of the other methods incorporate it. Tables IV and V present the results of our comparison on the IEEE 906-node system with the maximum throughput objective, considering 25% and 75% consumer participation, respectively. These tables demonstrate the average total injected real energy (ATIRE) for 1000 scenarios per time step, the average total number of voltage violations (ATNVV) per scenario, and the maximum voltage magnitude in the worst-case scenario. In the 75% consumer participation case, the commonly used 5 kW fixed export limit (FEL) fails to ensure network security, with an average of 775 voltage violations during our study horizon. The maximum voltage magnitude in the worst-case scenario using the FEL approach in this case exceeds 1.12 pu, far exceeding the allowable 1.05 pu voltage limit. In contrast, the FEL approach does not create any voltage violation problems in the case of 25% participation. However, it does result in a decrease in injection power compared to our approach.

We observe that using OFEL and DEL approaches to

[9]The operating envelopes are primarily restricted by the network physical characteristics such as line resistance, reactance, and the thermal limits of transformers and conductors. These constraints remain relatively constant as long as the network infrastructure remains unchanged. In this paper, we adopted a one-year timeframe with an hourly resolution to simulate the operational phase and showcase the impact of demand response.

Table IV
BENCHMARK AGAINST ALTERNATIVE APPROACHES IN THE 906-NODE NETWORK WITH 25% CONSUMER PARTICIPATION.

| Approach / Objective | | ATIRE (MWh) | ATNVV | MVWC (pu) |
|---|---|---|---|---|
| Proposed | Reg 1 | 1689.3 | 0 | 1.05 |
| | Reg 2 | 1689.3 | 0 | 1.05 |
| 5kW FEL | | 393.8 | 0 | 1.03 |
| OFEL ($\overline{p}$) | | 760.2 | 4 | 1.06 |
| DEL ($\overline{p}_t$) | | 934.4 | 7 | 1.07 |

Table V
BENCHMARK AGAINST ALTERNATIVE APPROACHES IN THE 906-NODE NETWORK WITH 75% CONSUMER PARTICIPATION.

| Approach / Objective | | ATIRE (kWh) | ATNVV | MVWC (pu) |
|---|---|---|---|---|
| Proposed | Reg 1 | 1821.4 | 0 | 1.05 |
| | Reg 2 | 1821.4 | 0 | 1.05 |
| 5kW FEL | | 2223.9 | 775 | 1.12 |
| OFEL ($\overline{p}$) | | 561.1 | 11 | 1.08 |
| DEL ($\overline{p}_t$) | | 688.6 | 22 | 1.08 |

Table VI
SUMMARY OF THE INSTALLED PV SYSTEMS, AND THE TOTAL INVESTMENT AND OPERATIONAL COSTS IN THE 906-NODE NETWORK WITH 75% CONSUMER PARTICIPATION. INVESTMENT COSTS ARE ANNUALISED FOR CONSISTENCY WITH OPERATIONAL EXPENSES.

| Approach / Objective | | Inst. PV | Inv. cost ($) | Op. cost ($) |
|---|---|---|---|---|
| Proposed | Reg 1 | 366 | 29220 | -1097 |
| | Reg 2 | 366 | 29220 | -1097 |
| 5kW FEL | | 475 | 36506 | -18726 |
| OFEL ($\overline{p}$) | | 124 | 13113 | 54103 |
| DEL ($\overline{p}_t$) | | 144 | 14453 | 48519 |

calculate the upper bound for a fixed export limit might endanger network's security[10]. In the worst-case scenario, these approaches resulted in voltage violations as high as 0.03 p.u. in our study. While the DEL approach performs slightly better than the OFEL in terms of total injected real energy, they result in more voltage violations.

Table VI reports the installed DER capacity and a detailed breakdown of investment and operational costs associated with employing the maximum throughput objective. The reported values denote the installation sizes of DER systems in kilowatts (kW), and all costs are presented in AU dollars ($). The results indicate that the FEL approach yielded the highest installation of DER systems. However, considering this outcome with the number of voltage violations presented in Table V, it becomes evident that this approach overestimates the network hosting capacity, leading to compromised network security and the potential disconnection of DER systems. This translates to a waste of investment made by DER owners, as their assets could be compelled to disconnect from the grid multiple times throughout the year. We can also see that our proposed approaches better use network capacity by installing more DER systems and reducing the consumers' total costs relative to OFEL and DEL approaches.

## VI. Limitations and Considerations

As the number of participating consumers grows, the allocated DOEs per consumer decrease in size. This trend is evident in our numerical experiments depicted in Fig. 7. Furthermore, a comparison between the DOEs in Fig. 5 and Fig. 8 indicates that as consumers connect to the grid at greater electrical distances from the upstream transformer, the sizes of their DOEs diminish. These outcomes are expected since DOEs essentially distribute the remaining network capacity among participating consumers. In cases where there is a substantial increase in the number of participants, the DOEs may impose overly restrictive operating conditions on consumers, presenting them with new challenges in meeting their allocated DOEs. Consequently, intervention from the DSO may become necessary. The DSO can implement bilateral contracts to selectively restrict certain consumers more than others, ensuring that the remaining network capacity remains available for other consumers. Alternatively, network operators can explore network upgrade options, granting consumers greater flexibility to invest in behind-the-meter DER installations.

In our network problem, we are solving an optimisation problem to maximise the network throughput using a linearised power flow model around the no-load condition. The rationale for selecting this condition is that the value of the DER systems' sizes are not known ahead of time. Thus, we do not have access to their generation/consumption before solving the optimisation problem. Finding a more suitable operating point to linearise the power flow equation in a planning OPF problem is not trivial and falls beyond the boundaries of our current study. We have left using a more accurate power flow model to future work.

[10]Using an OPF to obtain the upper fixed export limit is only valid for single-phase networks. In three-phase systems, negative mutual impedances mean that a reduction in injection at one node can increase the voltage magnitude at another node. Although cases of negative impedance in LV networks, to the degree where a reduction in power injection would lead to more overvoltages, are rare in practice, it is imperative for system operators to be aware of this possibility, particularly when employing multiple OPFs to determine a DOE for a given node. This phenomenon has been thoroughly investigated in [43].

## VII. Conclusions

This paper introduces a hierarchical optimization framework for assessing DER capacity in active distribution systems. The framework decomposes the power grid and consumer problems, connected through a dynamic operating envelope. The DOE is defined as a convex set that includes an acceptable range of real and reactive power flows for each consumer's connection point, within each operational interval that complies with network constraints.

To calculate the DOEs, we propose a novel methodology based on the right-hand side (Kornai–Liptak) decomposition technique. This approach ensures that each flexible node contributes to keeping operational limits within acceptable ranges with a specific weight. We present two regularisation terms to obtain these weights. In the first term, flexible nodes/consumers contribute equally, while in the second term, they contribute based on their sensitivities. To demonstrate the effectiveness of our approach, we conduct numerical experiments on the IEEE 37-node and 906-node test systems. Our approach successfully maintains network security while protecting consumer agency.

## Appendix

This section details the consumer problem reformulation using the AARC methodology.

Let vector $\boldsymbol{x}$ denote the decision variables, e.g. inverter and battery size and their real and reactive power injections. Also, let $\boldsymbol{\xi}$ be the random vector, collecting the PV efficiency coefficient and electrical demand deviations from their predicted values. Let the random vector $\boldsymbol{\xi}$ be supported on the polyhedral uncertainty set $\mathcal{U} := \{\boldsymbol{\xi} | \mathbf{M}\boldsymbol{\xi} \leq \mathbf{m}\}$, where $\mathbf{m}$ and $\mathbf{M}$ are the corresponding constant parameters. Let functions $f'(\boldsymbol{x}, \boldsymbol{\xi})$ and $f''(\boldsymbol{x}, \boldsymbol{\xi})$ denote the objective function and the set of constraints in the consumer problem, respectively. Also, let operator $\mathbb{E}[.]$ denotes the expected value of the corresponding vector. The consumer problem can then be written in the following abstract form:

$$\min_{x} \ \mathbb{E}[f'(\boldsymbol{x}, \boldsymbol{\xi})] \tag{39a}$$

$$f''(\boldsymbol{x}, \boldsymbol{\xi}) \leq 0 \quad \forall \boldsymbol{\xi} \in \mathcal{U}. \tag{39b}$$

In what follows, we reformulate the uncertain optimisation problem (39) to a linear program. First, we employ the sample average approximation method [44] to estimate the expected value of the objective function by averaging it over a limited set of samples, as shown below:

$$\mathbb{E}[f'(\boldsymbol{x}, \boldsymbol{\xi})] = \frac{1}{|\mathcal{S}|} \sum_{s \in \mathcal{S}} f'(\boldsymbol{x}, \boldsymbol{\xi}^s) \tag{40}$$

where superscript $s$ denotes evaluated value at the $s$-th sample point in the sample space $\mathcal{S}$.

Next, we employ the AARC methodology to deal with constraint (39b). Based on AARC, we can partition our decision variable vector $\boldsymbol{x}$ to two vectors; those that must be determined before the realisation of uncertain parameters $\boldsymbol{\xi}$ and those that can be update after the uncertainty realisation. In our context, the PV and battery size belong to the first partition and their real and reactive power injection belong to the second one. We will refer to these two vectors with $\boldsymbol{x}^u$ and $\boldsymbol{x}^a$, respectively. Next, AARC enforces that $\boldsymbol{x}^a$ should be an affine function of the uncertain, i.e., $\boldsymbol{x}^a = \boldsymbol{\alpha}\boldsymbol{\xi} + \boldsymbol{x}^{\mathbf{0}}$, where $\boldsymbol{\alpha}$ and $\boldsymbol{x}^{\mathbf{0}}$ are parameters of the affine function and new variables of the optimisation. Therefore, constraint (39b) can be rewritten as follows:

$$\boldsymbol{g}_1(\boldsymbol{x}^u, \boldsymbol{\alpha})\, \boldsymbol{\xi} + \boldsymbol{g}_0(\boldsymbol{x}^u, \boldsymbol{x}^{\mathbf{0}}) \leq 0, \quad \forall \boldsymbol{\xi} \in \mathcal{U} \tag{41}$$

where $\boldsymbol{g}_1$ and $\boldsymbol{g}_0$ are linear functions in their arguments. We then use the robust optimisation approach and the the duality technique described in [23] to reformulate (39b) as a linear constraint that as robust against any realisation of $\boldsymbol{\xi}$ within the uncertainty set $\mathcal{U}$. The reformulated constraints are written as:

$$\boldsymbol{m}^\intercal \boldsymbol{\lambda} \leq -\boldsymbol{g}_0(\boldsymbol{x}^u, \boldsymbol{x}^{\mathbf{0}}),\ \boldsymbol{M}^\intercal \boldsymbol{\lambda} \geq \boldsymbol{g}_1(\boldsymbol{x}^u, \boldsymbol{\alpha}) \tag{42}$$

where $\boldsymbol{\lambda}$ is the vector of dual variables associated with the bounding constraints in the uncertainty set $\mathcal{U}$.

To summarise, we used the AARC methodology to reformulate the uncertain optimisation problem (39) with a linear program with objective (40) and subject to constraint (42).

## REFERENCES


[1] S. Abapour, K. Zare, and B. Mohammadi-Ivatloo, "Maximizing penetration level of distributed generations in active distribution networks," in *2013 Smart Grid Conference (SGC)*. IEEE, 2013, pp. 113–118.

[2] S. Wang, S. Chen, L. Ge, and L. Wu, "Distributed generation hosting capacity evaluation for distribution systems considering the robust optimal operation of OLTC and SVC," *IEEE Transactions on Sustainable Energy*, vol. 7, no. 3, pp. 1111–1123, 2016.

[3] B. Wang, C. Zhang, Z. Y. Dong, and X. Li, "Improving hosting capacity of unbalanced distribution networks via robust allocation of battery energy storage systems," *IEEE Transactions on Power Systems*, vol. 36, no. 3, pp. 2174–2185, 2020.

[4] M. Mahmoodi, A. Attarha, S. M. N. RA, P. Scott, and L. Blackhall, "Adjustable robust approach to increase DG hosting capacity in active distribution systems," *Electric Power Systems Research*, vol. 211, p. 108347, 2022.

[5] H. Al-Saadi, R. Zivanovic, and S. F. Al-Sarawi, "Probabilistic hosting capacity for active distribution networks," *IEEE Transactions on Industrial Informatics*, vol. 13, no. 5, pp. 2519–2532, 2017.

[6] R. Gupta, F. Sossan, and M. Paolone, "Countrywide PV hosting capacity and energy storage requirements for distribution networks: The case of switzerland," *Applied Energy*, vol. 281, p. 116010, 2021.

[7] S. Boyd, N. Parikh, and E. Chu, *Distributed optimization and statistical learning via the alternating direction method of multipliers*. Now Publishers Inc, 2011.

[8] A. Attarha, P. Scott, and S. Thiébaux, "Affinely adjustable robust ADMM for residential DER coordination in distribution networks," *IEEE Transactions on Smart Grid*, vol. 11, no. 2, pp. 1620–1629, 2019.

[9] K. Petrou, M. Z. Liu, A. T. Procopiou, L. F. Ochoa, J. Theunissen, and J. Harding, "Managing residential prosumers using operating envelopes: An australian case study," in *Proceedings of the CIRED Workshop, Berlin, Germany*, 2020, pp. 22–23.

[10] S. M. N. R. Abadi, M. Mahmoodi, P. Scott, L. Blackhall, and S. Thiébaux, "Active management of LV residential networks under high PV penetration," in *2019 IEEE Milan PowerTech*. IEEE, 2019, pp. 1–6.

[11] M. Mahmoodi, S. M. N. RA, A. Attarha, L. Blackhall, and J. Hendriks, "Impact assessment of active network management schemes on dg capacity of distribution systems," in *2022 IEEE International Conference on Power Systems Technology (POWERCON)*. IEEE, 2022, pp. 1–7.

[12] "EVOLVE DER Project: On the calculation and use of dynamic operating envelopes," *Available: https://arena.gov.au/projects/evolve-der-project/*.

[13] "EVOLVE project m4 knowledge sharing report: On the calculation and use of dynamic operating envelopes."

[14] A. Attarha, S. M. N. RA, P. Scott, and S. Thiébaux, "Network-secure envelopes enabling reliable DER bidding in energy and reserve markets," *IEEE Transactions on Smart Grid*, 2021.

[15] J. Silva, J. Sumaili, R. J. Bessa, L. Seca, M. Matos, and V. Miranda, "The challenges of estimating the impact of distributed energy resources flexibility on the tso/dso boundary node operating points," *Computers & Operations Research*, vol. 96, pp. 294–304, 2018.

[16] J. Silva, J. Sumaili, R. J. Bessa, L. Seca, M. A. Matos, V. Miranda, M. Caujolle, B. Goncer, and M. Sebastian-Viana, "Estimating the active and reactive power flexibility area at the tso-dso interface," *IEEE Transactions on Power Systems*, vol. 33, no. 5, pp. 4741–4750, 2018.

[17] M. Kalantar-Neyestanaki, F. Sossan, M. Bozorg, and R. Cherkaoui, "Characterizing the reserve provision capability area of active distribution networks: A linear robust optimization method," *IEEE Transactions on Smart Grid*, vol. 11, no. 3, pp. 2464–2475, 2019.

[18] F. Capitanescu, "TSO–DSO interaction: Active distribution network power chart for TSO ancillary services provision," *Electric Power Systems Research*, vol. 163, pp. 226–230, 2018.

[19] K. Petrou, A. T. Procopiou, L. Gutierrez-Lagos, M. Z. Liu, L. F. Ochoa, T. Langstaff, and J. Theunissen, "Ensuring distribution network integrity using dynamic operating limits for prosumers," *IEEE Transactions on Smart Grid*, 2021.

[20] A. Attarha, P. Scott, and S. Thiébaux, "Network-aware co-optimisation of residential DER in energy and FCAS markets," *Electric Power Systems Research*, vol. 189, p. 106730, 2020.

[21] J. Kornai and T. Liptak, "Two-level planning," *Econometrica: Journal of the Econometric Society*, pp. 141–169, 1965.

[22] I. V. Konnov, "Right-hand side decomposition for variational inequalities," *Journal of Optimization Theory and Applications*, vol. 160, no. 1, pp. 221–238, 2014.

[23] S. Boyd and L. Vandenberghe, *Convex optimization*. Cambridge university press, 2004, pp. 215–273.

[24] A. Ben-Tal, A. Goryashko, E. Guslitzer, and A. Nemirovski, "Adjustable robust solutions of uncertain linear programs," *Mathematical programming*, vol. 99, no. 2, pp. 351–376, 2004.

[25] J. Nocedal and S. J. Wright, *Numerical optimization*. Springer, 1999.

[26] S. M. N. RA, M. Burgess, M. Mahmoodi, A. Attarha, and P. Scott, "An adjustable scenario optimisation approach in operating pv-rich distribution systems," *IEEE Transactions on Power Systems*, 2022.

[27] M. Vanin, H. Ergun, R. D'hulst, and D. Van Hertem, "Comparison of linear and conic power flow formulations for unbalanced low voltage network optimization," *Electric Power Systems Research*, vol. 189, p. 106699, 2020.

[28] S. M. N. RA, P. Scott, M. Mahmoodi, and A. Attarha, "Data-driven adjustable robust solution to voltage-regulation problem in pv-rich distribution systems," *International Journal of Electrical Power & Energy Systems*, vol. 141, p. 108118, 2022.

[29] K. Girigoudar and L. A. Roald, "On the impact of different voltage unbalance metrics in distribution system optimization," *Electric Power Systems Research*, vol. 189, p. 106656, 2020.

[30] M. Mahmoodi and L. Blackhall, "DER hosting capacity envelope in unbalanced distribution systems," in *2021 IEEE PES Innovative Smart Grid Technologies Europe (ISGT Europe)*. IEEE, 2021, pp. 1–6.

[31] S. Bolognani and S. Zampieri, "On the existence and linear approximation of the power flow solution in power distribution networks," *IEEE Transactions on Power Systems*, vol. 31, no. 1, pp. 163–172, 2015.

[32] L. Gurobi Optimization, "Gurobi optimizer reference manual," 2020. [Online]. Available: http://www.gurobi.com

[33] R. A. Jabr, "Robust volt/var control with photovoltaics," *IEEE Transactions on Power Systems*, vol. 34, no. 3, pp. 2401–2408, 2019.

[34] M. Shaw, B. Sturmberg, L. Guo, X. Gao, E. Ratnam, and L. Blackhall, "The NextGen energy storage trial in the ACT, Australia," in *Proceedings of the Tenth ACM International Conference on Future Energy Systems*, 2019, pp. 439–442.

[35] S. Pfenninger and I. Staffell, "Long-term patterns of European PV output using 30 years of validated hourly reanalysis and satellite data," *Energy*, vol. 114, pp. 1251–1265, 2016.

[36] M. Mahmoodi, M. Shaw, and L. Blackhall, "Voltage behaviour and distribution network performance with community energy storage systems and high PV uptake," in *Proceedings of the Eleventh ACM International Conference on Future Energy Systems*, 2020, pp. 388–390.

[37] "ACT electricity time-of-use tariff." *[Online]. Available: https://actewagl.com.au/ /media/actewagl/actewagl-files/products-and-services/retail-prices/electricity-retail-prices/act-electricity-schedule-of-charges-2017-18.pdf,.*

[38] "Rooftop solar capital cost per kw installation." *[Online]. Available: https://www.solarquotes.com.au/panels/cost/,.*

[39] "Housesohold battery capital cost per kwh installation." *[Online]. Available: https://reneweconomy.com.au/household-battery-storage-costs-so-near-and-yet-so-far-48870/,.*

[40] Y. Xu, Z. Y. Dong, R. Zhang, and D. J. Hill, "Multi-timescale coordinated voltage/var control of high renewable-penetrated distribution systems," *IEEE Transactions on Power Systems*, vol. 32, no. 6, pp. 4398–4408, 2017.

[41] Y. Wu, S. M. Aziz, and M. H. Haque, "Techno-economic modelling for energy cost optimisation of households with electric vehicles and renewable sources under export limits," *Renewable Energy*, vol. 198, pp. 1254–1266, 2022.

[42] T. R. Ricciardi, K. Petrou, J. F. Franco, and L. F. Ochoa, "Defining customer export limits in PV-rich low voltage networks," *IEEE Transactions on Power Systems*, vol. 34, no. 1, pp. 87–97, 2018.

[43] B. Liu and J. H. Braslavsky, "Sensitivity and robustness issues of operating envelopes in unbalanced distribution networks," *IEEE Access*, vol. 10, pp. 92 789–92 798, 2022.

[44] A. J. Kleywegt, A. Shapiro, and T. Homem-de Mello, "The sample average approximation method for stochastic discrete optimization," *SIAM Journal on optimization*, vol. 12, no. 2, pp. 479–502, 2002.